

2017

Design of flow cytometry panels to investigate killer immunoglobulin-like receptor expressing lymphocytes in ankylosing spondylitis

<https://hdl.handle.net/2144/23810>

"Downloaded from OpenBU. Boston University's institutional repository."

BOSTON UNIVERSITY
SCHOOL OF MEDICINE

Thesis

**DESIGN OF FLOW CYTOMETRY PANELS TO INVESTIGATE KILLER
IMMUNOGLOBULIN-LIKE RECEPTOR EXPRESSING LYMPHOCYTES IN
ANKYLOSING SPONDYLITIS**

by

JOHN S. LEE

B.A., University of California, San Diego, 2013

Submitted in partial fulfillment of the
requirements for the degree of
Master of Science

2017

© 2017 by
John S. Lee
All rights reserved

Approved by

First Reader

Karen Symes, Ph.D.
Associate Professor of Biochemistry

Second Reader

Joerg Ermann, M.D.
Brigham and Women's Hospital

ACKNOWLEDGEMENTS

I wish to thank Joerg Ermann for his constant support, guidance, and mentorship throughout the entirety of this project. I am grateful for the kindness and patience that he has shown me while teaching me about laboratory science techniques and concepts. I also wish to acknowledge Imtiyaz Hossain for teaching me several indispensable techniques, and for his advice with technical issues and laboratory procedures. Finally, I thank the other members of the Charles-Ermann Laboratory, Julia Charles, Jing Yan, Kelly Tsang, Haoming Liu, and Belinda Beqo, for their help and advice throughout this project.

**DESIGN OF FLOW CYTOMETRY PANELS TO INVESTIGATE KILLER
IMMUNOGLOBULIN-LIKE RECEPTOR EXPRESSING LYMPHOCYTES IN
ANKYLOSING SPONDYLITIS**

JOHN S. LEE

ABSTRACT

The major histocompatibility complex (MHC) class I molecule, Human Leukocyte Antigen B27 (HLA-B27) is a strong genetic risk factor for Ankylosing Spondylitis (AS). However, the mechanism linking HLA-B27 and the development of AS is unknown. Recent studies have shown that monoclonal antibodies targeting interleukin 17A (IL-17A) are an effective therapy for many patients with AS suggesting that IL-17A secreting lymphocytes mediate the disease. Published experimental evidence suggests further a potential role for 4 specific killer cell immunoglobulin-like receptors (KIRs) in the pathogenesis of AS, namely KIR3DL1, KIR3DL2, KIR2DL5, and KIR3DS1. KIRs are immunomodulatory receptors for MHC class I molecules that are expressed by a variety of lymphocyte subsets. We hypothesize that the expression of these AS-associated KIRs differentially modulates the expression of IL-17A in HLA-B27 positive vs. negative individuals thereby affecting susceptibility to AS. To begin to address this hypothesis, the experiments described in thesis were performed

to develop a set of multi-color flow cytometry panels that permit the analysis of expression of KIR3DL1, KIR3DL2, KIR2DL5, KIR3DS1 and of IL-17A by major classical and unconventional lymphocytes subsets. These panels will be used in future studies to analyze peripheral blood samples from genotyped HLA-B27 positive and negative healthy individuals as well as from AS patients and controls.

TABLE OF CONTENTS

TITLE.....	i
COPYRIGHT PAGE.....	ii
READER APPROVAL PAGE.....	iii
ACKNOWLEDGEMENTS	iv
ABSTRACT	v
TABLE OF CONTENTS	vii
LIST OF TABLES	viii
LIST OF FIGURES	ix
LIST OF ABBREVIATIONS	x
INTRODUCTION	1
METHODS.....	17
RESULTS	21
DISCUSSION	35
REFERENCES.....	39
CURRICULUM VITAE	45

LIST OF TABLES

Table	Title	Page
1	Antibody List.	21
2	Finalized flow panels for cell surface marker staining.	26
3	Finalized flow panels for intracellular cytokines.	27

LIST OF FIGURES

Figure	Title	Page
1	Activating and Inhibitory Killer Cell Immunoglobulin-Like Receptors.	5
2	IL-23 Signaling Leading to IL-17A Production In Various Cell Populations.	8
3	Lymphocyte Hierarchy.	12
4	Flow Cytometer Overview.	13
5	The Problem of Spectral Overlap.	16
6	Bead Compensation.	22
7	Antibody Titration and Corresponding Fluorescence Signal Strength.	22
8	Managing the Problem of CD4 Downregulation.	28
9	Gating Strategy.	31
10	The Use of Combinatorial Staining To Identify KIR3DL2+ Cells.	32
11	Variable KIR Expression on Different Lymphocyte Subsets.	33

LIST OF ABBREVIATIONS

AS.....	Ankylosing Spondylitis
APC.....	Allophycocyanin
BV.....	Brilliant Violet
CCR.....	Chemokine Receptor
CD.....	Cluster of Differentiation
EDTA.....	Ethylenediaminetetraacetic Acid
ER.....	Endoplasmic Reticulum
FACS.....	Fluorescence-Activated Cell Sorting
FBS.....	Fetal Bovine Serum
FITC.....	Fluorescein Isothiocyanate
FVD.....	Fixable Viability Dye
HBSS.....	Hank's Balanced Salt Solution
HLA.....	Human Leukocyte Antigen
HLA-DR.....	Human Leukocyte Antigen-Antigen D Related
IC.....	Intracellular
IFN- γ	Interferon- γ
IL-17A.....	Interleukin-17A
IL-23R.....	Interleukin-23 Receptor
Io.....	Ionomycin
ITIM.....	Immunoreceptor Tyrosine-based Activation Motif

ITIM	Immunoreceptor Tyrosine-based Inhibitory Motif
KIR	Killer Cell Immunoglobulin-Like Receptor
MAIT	Mucosal Associated Invariant T-Cell
MHC	Major Histocompatibility Complex
NFAT	Nuclear Factor of Activated T-Cells
NK	Natural Killer
PBMC	Peripheral Blood Mononuclear Cell
PE	Phycoerythrin
PerCP	Peridinin Chlorophyll Protein
RPM	Rotations Per Minute
RPMI-C	Roswell Park Memorial Institute-Complete
TCR	T-Cell Receptor
UPR	Unfolded Protein Response
UV	Ultraviolet
$\gamma\delta$ TCR	Gamma Delta T-Cell Receptor
β 2m	Beta 2-Microglobulin

INTRODUCTION

Ankylosing spondylitis (AS) is a form of chronic arthritis, primarily affecting the sacroiliac joints and the spine. AS usually affects younger male patients from 15 to 30 years of age. The cause of AS is largely unknown, but there is strong evidence that the gene HLA-B27 plays a direct role in increasing susceptibility to AS.¹ Patients with AS suffer from severe back pain and stiffness, in particular in the morning. Moreover, many AS patients develop deformities in their back due to the fusion of vertebrae. Over time, this causes a hunched back and affects the mobility of the individual. The ankylosed spine is also prone to fracture.

In addition, this disease has been known to cause inflammation in the peripheral joints, eyes and promote new bone formation in affected areas. Unfortunately, there is no cure for this disease but there have been treatments that target specific inflammatory cytokines to reduce pain and inflammation.² Between 0.1% to 1.8% of people are affected, making it as common as rheumatoid arthritis.¹

HLA-B27 and its Association with AS

HLA-B27 is one of the many Major Histocompatibility Complex (MHC) Class I molecules that is responsible for presenting endogenous peptides to lymphocytes, specifically to CD8+ cytotoxic T-cells. Structurally, the MHC class I heavy chains form a heterotrimeric complex with β 2-microglobulin (β 2m) and a

short peptide of 8-10 amino acids. This complex is generated inside of the endoplasmic reticulum (ER). Once this complex is fully assembled, it is transported to the cell surface, where it is then recognized by other cells.²

In the early 1970s, serological procedures that were initially used for tissue typing organ transplantations were adopted in rheumatological research. This led to the discovery of the association between HLA-B27 and AS.³ HLA-B27 was the first HLA allele that was found to have an association with an inflammatory disease and was also shown to be associated with other spondyloarthropathies like reactive arthritis, psoriatic arthritis, and uveitis.⁴ Almost 90% of people with AS are HLA-B27 positive.⁵ Although the association between HLA-B27 and AS is very strong, the presence of HLA-B27 alone is not sufficient to induce disease.

Hypotheses for the Association between HLA-B27 and AS

There are currently four major hypotheses that attempt to explain the association between HLA-B27 and AS.

- 1) ***Arthritogenic/spondylitogenic peptide hypothesis:*** This hypothesis refers to the well-established MHC class I function of HLA-B27, which is antigen presentation to CD8+ T cells. It is postulated that activation of cytotoxic CD8+ T-cells and subsequent cell-mediated immune responses against specific HLA-B27/peptide combinations lead to disease.⁶

- 2) **Misfolding hypothesis:** HLA-B27 has a unique property in that HLA-B27 heavy chains have a tendency to misfold during assembly of the heterotrimeric complex of the HLA-B27 heavy chain, β 2m, and peptide in the ER. Accumulation of these misfolded proteins within the ER has been demonstrated to illicit a cellular stress response known as unfolded protein response (UPR), which comprises a number of pathways, all involved in decreasing the amount of misfolded protein aggregation within in the ER. Activation of the UPR can also lead to inflammation.⁷
- 3) **Homodimer/NK cell receptor hypothesis:** Another unique property of HLA-B27 is that HLA-B27 molecules may form disulfide linked homodimers, which do not need the presence of β 2m or peptide for expression on the cell surface. After this discovery, it was found that KIR3DL2, an inhibitory NK cell receptor, displayed a stronger affinity for the aforementioned HLA-B27 heavy chain homodimer than for regular HLA-B27 complexes. Interestingly, NK cell receptors like KIR3DL2 are not exclusively expressed on NK cells. It has been shown that HLA-B27 heavy chain homodimers may induce the inappropriate activation of CD4+ T-cells expressing KIR3DL2.²
- 4) **Microbial hypotheses:** The results from multiple studies implicate microbes in the pathogenesis of AS and other HLA-B27 associated diseases. These lines of evidence include the induction of reactive arthritis by certain Gram-negative bacteria, the high prevalence of

intestinal inflammation in patients with AS, and the importance of microbiota for the development of arthritis in HLA-B27 transgenic rats. Microbial hypotheses to explain the association of HLA-B27 and AS invoke immunological cross-reactivity, compromised immunological defenses against certain microbes in HLA-B27+ individuals, or indirect consequences involving intestinal microbiota.⁸

Each of the 4 hypotheses has its strengths and weaknesses and, despite extensive research efforts, the exact mechanism linking HLA-B27 and AS is still unknown.

Killer Cell Immunoglobulin-like Receptors

Killer cell immunoglobulin-like receptors are a family of type I transmembrane proteins that are expressed on the surface of NK cells and other types of lymphocytes.⁹ They are referred to as immunoglobulin-like because they share structural similarities with antibody molecules. KIRs can act as both activators and inhibitors of NK cell cytotoxicity through their interaction with MHC class I molecules expressed on the surface of nucleated cells.¹⁰ The function of KIRs on other lymphocytes is well understood.

Inhibitory KIRs have cytoplasmic tails with immunoreceptor tyrosine-based motifs (ITIM) that are phosphorylated when the receptors interact with MHC class I molecules. ITIM phosphorylation induces the activation of cytoplasmic tyrosine phosphatases that remove phosphate groups from tyrosine residues of various

signaling molecules. This prevents the activation of the KIR-expressing NK cell when the receptor interacts with self MHC molecules on healthy host cells.⁹

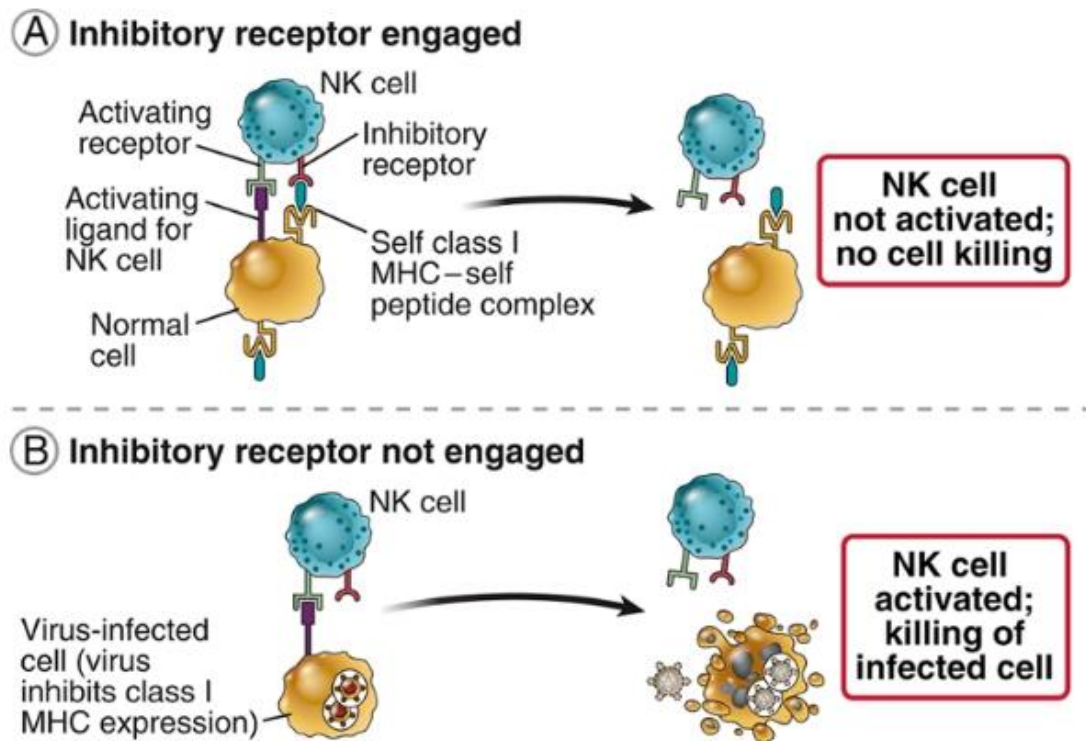


Figure 1. Activating and inhibitory killer cell immunoglobulin-like receptors. **A.** Inhibitory KIRs recognize MHC class I molecules expressed on normal host cells and ensure that these host cells are not attacked. **B.** Activating KIRs detect the presence of ligands on aberrant cells, in which class I MHC expression is usually reduced. This leads to NK cell activation and cytotoxicity. (Taken from Abbas).⁹

Activating KIRs detect ligands on the surface of abnormal cells and increase the cytotoxic activity of the KIR expressing NK cells. Activating KIRs do not have ITIMs, instead, they have positively charged arginine or lysine residues in their transmembrane domains that facilitate interaction with other membrane

proteins that have cytoplasmic immunoreceptor tyrosine-based activation motifs (ITAM) thereby promoting cell activation.¹¹

KIRs are encoded by the highly polymorphic KIR locus on Chromosome 19. Both the number and identity of KIR genes and the nucleotide sequences of individual KIR genes may differ between subjects. An additional source of heterogeneity is that KIRs are not uniformly expressed. Each NK cell or other KIR positive lymphocyte expresses only a selection the KIRs encoded by the subject's KIR genes.¹²

HLA-B27 and KIRs

Experimental evidence suggests a potential role for 4 KIRs in the pathogenesis of AS. KIR3DL1 has been shown to specifically interact with HLA-B27, an interaction that may be affected by the type of peptide bound to HLA-B27.¹³ KIR3DL2 does not bind well to the HLA-B28/ β 2m/peptide complex. Instead, KIR3DL2 has been shown to recognize HLA-B27 homodimers.¹⁴

As discussed above, homodimerization is a unique feature of the HLA-B27 heavy chain, and inappropriate activation of KIR3DL2 positive lymphocytes has been proposed as a mechanism linking HLA-B27 positivity and disease.¹⁵ Recent genetic studies have furthermore suggested a potential role for KIR3DS1 and KIR2DL5 in the pathogenesis of AS.¹⁶

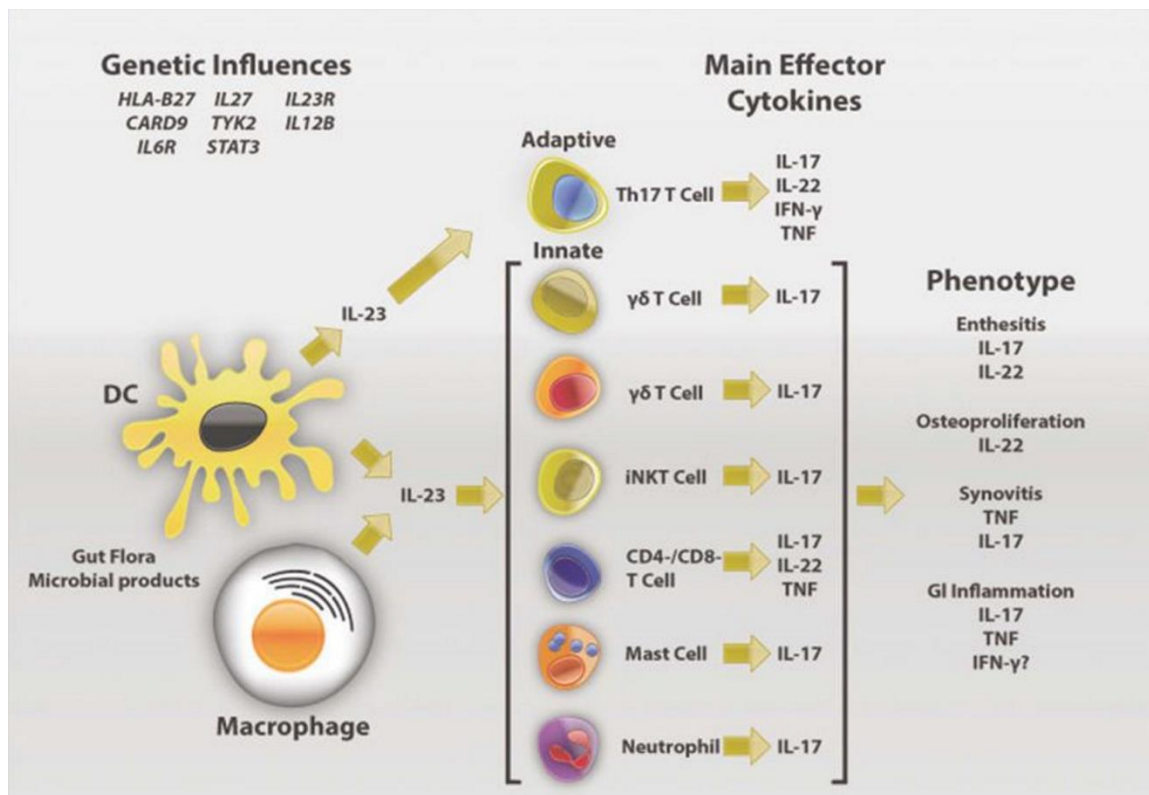


Figure 2. IL-23 signaling leading to IL-17A production in various cell populations. Signaling through the IL-23 receptor induces IL-17A production by multiple types of immune cells including $\gamma\delta$ Cells, iNKT-Cells, CD3+ T-Cells, CD4+ T-Cells, and NK Cells. (Taken from Smith).¹⁷

IL-23/IL-17A Axis in AS

Recent genome-wide association studies have demonstrated polymorphisms in several non-HLA genes to be associated with susceptibility to AS in Caucasian populations.¹⁸ In particular, polymorphisms in several genes involved in IL-23 receptor signaling were found to be associated with AS.¹⁹ IL-23 receptors are expressed on many immune cell, including CD4+ T-cells, $\gamma\delta$ T-cells, and NK cells. IL-23 receptor signaling induces the expression of IL-17A.¹⁷ IL-17A then acts on other types of cells to promote inflammatory responses. This

IL-23/IL-17A axis is thought to be important in the defense against microbes like bacteria, parasites, fungi, and viruses.²⁰

There is strong evidence that the IL-23/IL-17A cytokine axis plays a role in AS pathogenesis. Serum levels of IL-17A are higher in patients with AS compared with healthy subjects.¹⁷ Moreover, IL-17A inhibition has been shown to be an effective treatment for ankylosing spondylitis.²¹

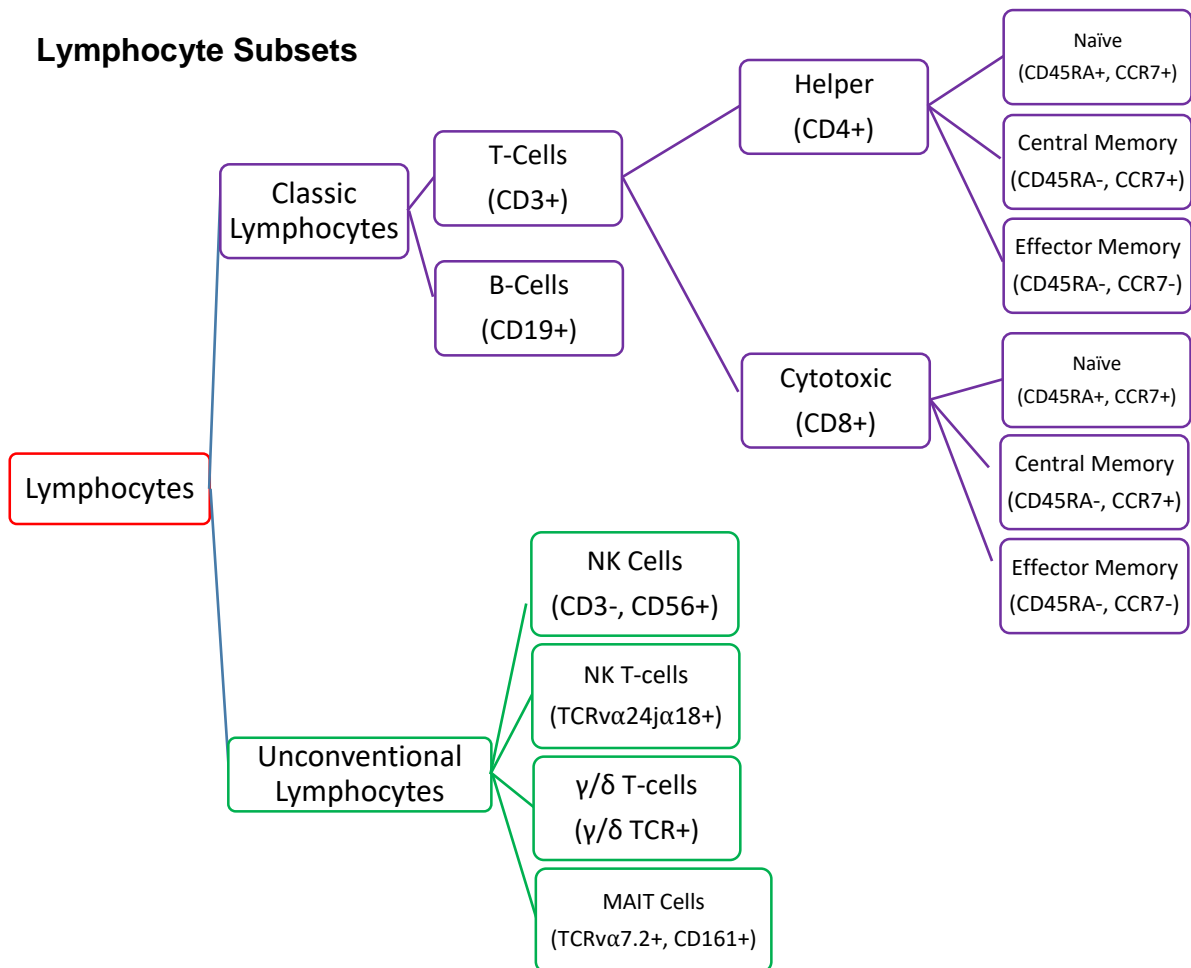


Figure 3. Lymphocyte hierarchy. Surface markers used to identify specific lymphocyte populations.^{22,23}

Multiple types of lymphocytes have been shown to secrete IL-17A including CD4+ T-cells, CD8+ T-cells, $\gamma\delta$ T-cells, NK cells, NK T-cells, and Mucosal Associated Invariant T-Cells (MAIT) cells. CD4+ helper and CD8+ cytotoxic T-cells are white blood cells that play a particularly important role in the adaptive immune system. CD4+ helper T-cells secrete cytokines that promote the phagocytic activity of macrophages, B-cell antibody class switching, and activation of CD8+ cytotoxic T-cells.²⁴ CD4+ helper T-cells are activated through the interaction of their T-cell receptors with MHC class II molecules that are expressed on the surface of antigen presenting cells like B-cells, dendritic cells, and macrophages.²⁵

CD8+ cytotoxic T-cells are lymphocytes that are involved in killing infected, damaged, or cancerous cells by releasing cytotoxins in response to activation via the interaction of their T-cell receptors and antigens presented by MHC class I molecules.²⁶

Unlike the α and β chains of the classical T-cell receptor, $\gamma\delta$ T-cells express a T-cell receptor that is composed of a γ chain and a δ chain. $\gamma\delta$ T-cells are found in relatively low numbers compared to other lymphocyte subsets in the skin, lungs, gut mucosa, and uterus and play a role in eliciting and carrying out immune responses.²⁷

Natural killer cells are part of the innate immune system. While T-cells interact with MHC molecules displayed on the surface of infected cells, causing the release of cytokine and induction of cytolysis or apoptosis, NK cells are

unique in that they can provide cytotoxic responses in the absence of “self” markers displayed by MHC class I molecules, resulting in much more rapid recognition and immune reactions.²⁸ NK T-cells are a heterogeneous family of immune cells that have characteristics of both NK cells and T-cells. NK T-cells express the invariant TCR α 24j α 18 and recognize lipids presented by CD1 molecules. The effector functions of these cells include the rapid activation of T-cells, B-cells, NK cells, dendritic cells, and macrophages.²⁹

MAIT cells are an unconventional subset of T-cells that express the invariant TCR α 7.2. MAIT cells recognize antigens presented by the non-classical MHC class I molecule MR1 and have been reported to have the unique role in controlling bacterial and yeast infections.³⁰

Peripheral Blood Mononuclear Cells

Peripheral blood mononuclear cells (PBMC) is an umbrella term that includes lymphocytes, monocytes, and other cells with a single round nucleus.³¹ In order to isolate PBMCs from whole blood, a technique called density gradient centrifugation is used. Whole blood samples are overlaid onto ficoll, a hydrophilic polysaccharide medium that, after centrifugation, separates the blood into a plasma layer, a PBMC layer, a polymorphonuclear cell layer, and a red blood cell layer. The PBMC layer can be isolated by pipetting the cells.³²

Phorbol 12-myristate 13-acetate and Ionomycin are used in conjunction to stimulate cytokine production by cells in vitro. PMA/Ionomycin serve to act as an

artificial stimulus that mimics TCR activation. PMA directly activates Protein Kinase C, a kinase downstream of ligand-receptor activation. Ionomycin is a calcium ionophore that can raise intracellular levels of calcium to induce Nuclear factor of activated T-cells (NFAT) signaling, and consequently up-regulate gene transcription.³³

Flow Cytometry and Fluorescence

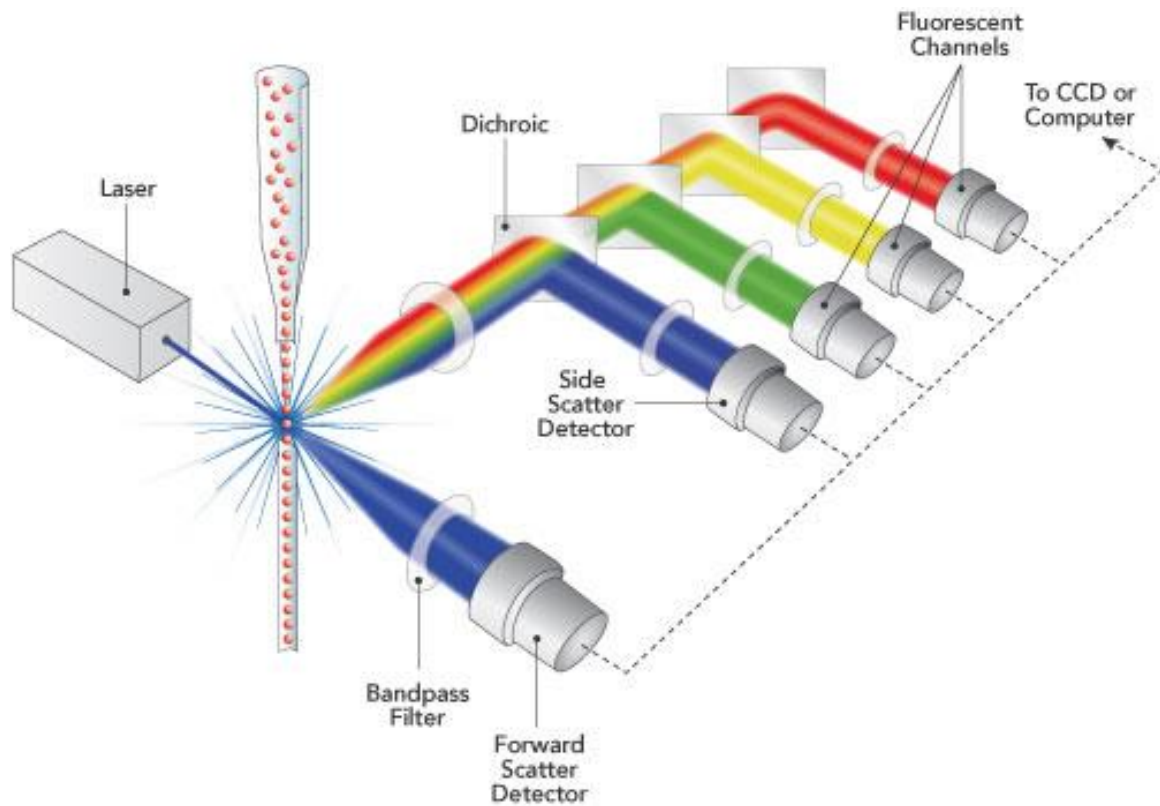


Figure 4. Flow cytometer overview. Laser light hits individual cells and scatter through different filters and are detected by a set of fluorescent channels. (Taken from Semrock).³⁴

Flow cytometry is used to identify subsets of cells within a heterogeneous population using different parameters like size, shape, and cell surface marker expression. Key components of flow cytometers are the fluidics system, lasers, detectors to sense the light, and a computer system to organize data for analysis.

Once a sample has been placed into the flow cytometer, the sample is taken in by the machine, mixed into a stream of sheath fluid and passed through a narrowing funnel that forces the cells into a single file line. This stream of single cells passes through several laser beams resulting in the scattering of light in a fashion that is dependent on the properties of each individual cell.³⁵

The two main forms of scattered light are forward and side scatter. The degree of forward scatter is proportional to the size of the cells and the degree of side scatter is proportional to the granularity of the cells. By analyzing the forward and side scatter together, the researcher can divide the heterogeneous populations of cells into individual populations with varying sizes, shapes, and complexities.³⁶

Fluorescence is a property of certain molecules called fluorophores that allows them to absorb light of short wavelengths and emit light of longer wavelengths. A flow cytometer can detect light emitted from excited fluorescent molecules like labeled antibodies. Monoclonal antibodies conjugated to fluorescent dyes, are used to identify the presence of different subsets of cells within heterogeneous samples because of their high specificity to surface markers on individual cells.³⁷ This high specificity coupled with laser induced

fluorophore excitation leads to the fluorescent signal that can then be detected and subsequently analyzed. The fluorophores are excited by a specific wavelength of laser light when the cells pass through the laser beams in the flow cytometer.³⁸ After excitation, the light emitted by the fluorophore is directed along a path with emission filters that filter out a light of a specific wavelength to be detected by sensors.³⁶ For example, a single 488 nm green laser that excites FITC and phycoerythrin (PE) was the laser used in the first two color flow cytometers.

There are many different classes of fluorophores including organic small molecules, proteins, semiconductor nanocrystals, and organic polymers. The diverse structures and chemical compositions of the different classes of fluorophores enable researchers to stain their samples with a variety of colors and identify many different markers at the same time.³⁹ Tandem dyes are composed of two covalently bonded fluorescent molecules, one of which acts as an excitation donor and the other as an acceptor. These fluorophores have the unique characteristics of having the excitation properties of the donor molecule and the emission properties of the acceptor molecule. By substituting different donor and acceptor molecules, new fluorophores can be designed.

More recently, the Brilliant Violet (BV) organic polymers have expanded the number of dyes that can be used in flow cytometry staining simultaneously. Unlike traditional UV-violet excitable dyes, the BV dyes are larger and have structural fluorescent repeats that act cooperatively to produce a stronger and

longer lasting signal similar to the strong staining of fluorophores like PE and allophycocyanin (APC).⁴⁰

The use of modern multicolor flow cytometers like the LSR Fortessa (BD Biosciences), that are equipped with 5 lasers (350 nm, 407 nm, 488 nm, 561 nm, 633 nm), enables the analysis of up to 18 colors simultaneously.⁴¹

Spectral Overlap and Compensation

Spectral overlap occurs when the fluorescence of a particular dye spills into more channels than the one that is expected to detect the dye's fluorescence.⁴² For example, FITC is a dye that emits primarily a green light that is measured in the FITC channel. FITC also emits a significant amount of yellow light, which is detected by the PE channel (Figure 5). This spectral overlap issue is amplified significantly when working with more colors. Fluorescence compensation is used to account for this spectral overlap. Compensation is the mathematical correction of the fluorescence signal intensities by applying a compensation matrix, which is generated by analyzing beads stained with single dyes. Compensation ensures that the fluorescent signal detected by each channel comes from the fluorophore that is getting measured and corrects any potential false positive signal caused by spillover.

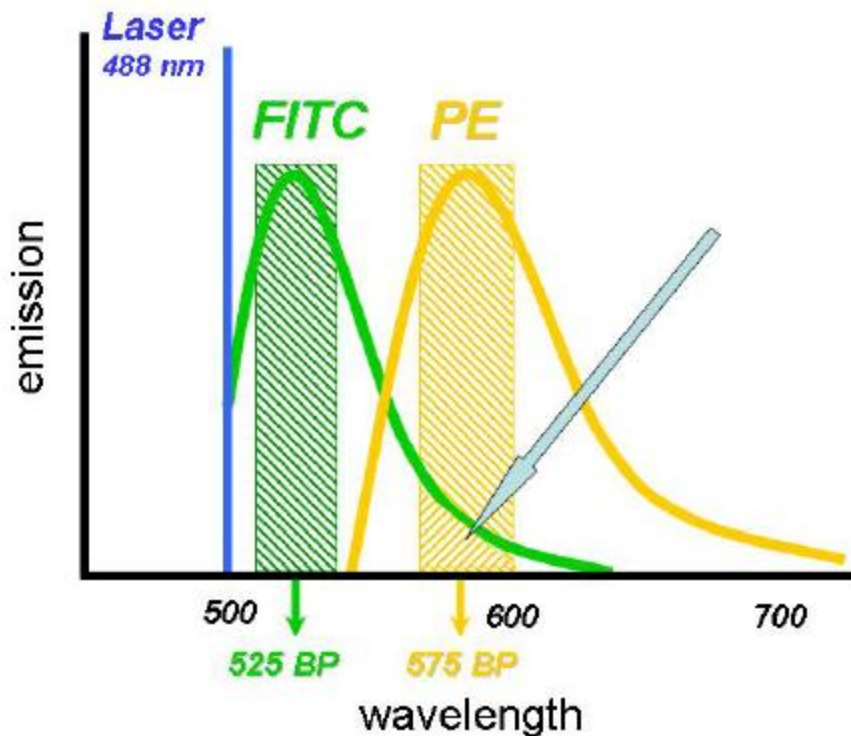


Figure 5. The problem of spectral overlap. Due to spectral overlap, the light emitted by FITC will be detected not only in the FITC channel but also in the PE channel. (Taken from Medical University of South Carolina).⁴³

Study Goals

Therapy with monoclonal antibodies or other biologics, targeting TNF or IL-17A has been shown to be effective for many patients with AS.²¹ Potential downsides of these therapies is that they are very expensive and leave patients vulnerable to the dangers of chronic immunosuppression.⁴⁴ As a result, there has been a greater emphasis on finding a cure and other preventative measures, both of which are unlikely to occur without a better grasp of the role HLA-B27 plays in AS pathogenesis. In this study, we wanted to design flow panels that

would allow the identification of the KIR repertoire on lymphocyte subsets and to see if there is a difference in the expression of these different lymphocyte subsets and their production of inflammatory cytokines. These studies in healthy individuals are critical prerequisites before analyzing specimen from patients who are HLA-B27+, HLA-B27-, and who have AS.

METHODS

Subjects

Blood samples were obtained from healthy volunteers and through the Crimson Cores program at Brigham and Women's Hospital. The Crimson Biomaterials Collection Core Facility collects discarded clinical blood samples and matches them to investigator-defined criteria. These samples are fully anonymized and were needed to increase the experiment's population size. The Crimson blood samples were necessary because we were interested in differential KIR expression on lymphocytes of different subjects and we were able to get many blood samples for little cost.

PBMC Isolation

Freshly collected human blood samples were processed within two hours of collection. 10 mL of anticoagulated blood was diluted with 14 mL of Hanks Balanced Salt Solution (HBSS) without Ca/Mg. We then added 15 mL of Ficoll-Paque (GE Healthcare) density medium into the insert of a SepMate-50 (STEMCELL Technologies) conical vial, overlaid the sample, and centrifuged at 2200 rpm for 20 minutes at room temperature with the brakes turned on. The PBMC layer was poured into a new 50 mL conical vial. The sample was then centrifuged at 1300 rpm for 10 minutes at 4° C. The resulting supernatant was aspirated and the cell pellet was resuspended and counted using Trypan Blue

(Life Technologies) cell viability dye and a Countess (Invitrogen) automated cell counter. The sample was centrifuged again at 1200 rpm for 10 minutes and resuspended in a volume associated with the desired cell concentration.

Cell Surface Staining

Surface marker staining was performed in 96 well plates. 150 μ L samples were put into wells of a 96-well round-bottom plate at a concentration of 2×10^6 cells/150 μ L. The cells were first stained with eFluor 455 UV fixable viability dye (1:500, 150 μ L per well) in HBSS for 15 minutes on ice. The cells were then washed with staining buffer [HBSS with 2mM Ethylenediaminetetraacetic Acid (EDTA) and 0.5% Bovine Serum Albumin (BSA)] and resuspended in staining buffer with Fc block (Biolegend, 1:100, 75 μ L per well) to inhibit non-specific binding of antibodies to Fc receptors on white blood cells. After a 10 minute incubation on ice fluorescently labeled antibodies diluted in Brilliant buffer (BD Biosciences) were added. The cells were incubated for 20 minutes on ice followed by two washes with staining buffer. If analysis was delayed, the cells were fixed with IC Fixation Buffer (eBioscience) for 10 minutes at room temperature and stored in a 4° C refrigerator in the dark. If the analysis occurred on the day of cell preparation, the cells were resuspended in 250 μ L of staining buffer and analyzed. A 5-laser, 20-parameter Fortessa flow cytometer (BD Biosciences) was used for data collection and FlowJo Software (FlowJo) was used for analysis.

Bead Compensation

On the day of analysis, UltraComp eBeads (eBioscience) were vortexed thoroughly in order to prevent sedimentation. A bead master mix was then prepared by mixing 250 μ L staining buffer to 10 μ L UltraComp beads per fluorescent channel. 250 μ L of the bead master mix was then aliquoted into individual FACS tubes. Antibodies were then added to the individual FACS tubes at a dilution of 1:500. These FACS tubes were then kept in the dark until analysis.

In vitro stimulation and intracellular staining.

2×10^6 Human PBMCs were added to individual wells of 96 well round-bottom plates in RPMI-C medium. Cells were placed in a 37° C incubator for 20 minutes prior to stimulation. Cells were stimulated with PMA/Ionomycin (eBioscience). Golgi Stop (BD Bioscience) was added to inhibit vesicle transport of cytokines. After four hours of incubation at 37° C, cells were harvested and stained for surface markers as described. After washing with staining buffer, the cells were fixed with IC Fixation Buffer (eBioscience) for 10 minutes at room temperature. After three washes with permeabilization buffer (eBioscience), anti-IL-17A antibody diluted in permeabilization buffer, was added for intracellular staining for another 30 minutes. This was followed by a series of washes with permeabilization buffer. The cells were then resuspended in staining buffer and analyzed.

Table 1. Antibody List.

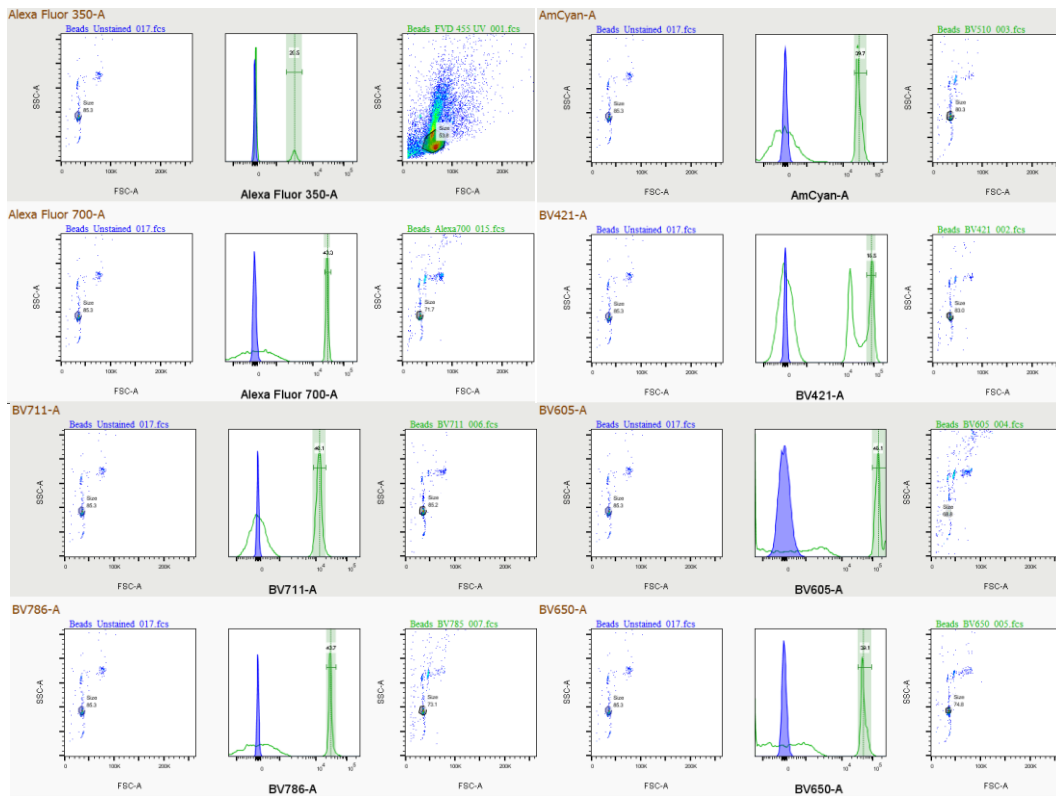
Dye	Target Name	Clone	Company
BV421	TCR α 24j α 18	6B11	Biolegend
	CCR7	G043H7	Biolegend
BV510	CD4	OKT4	Biolegend
	IL-17A	BL168	Biolegend
BV605	TCR α 7.2	3C10	Biolegend
	HLA-DR	L243	Biolegend
BV650	CD16	3G8	Biolegend
	IFN γ	4S.B3	Biolegend
	CD38	HB7	Biolegend
BV711	CD8a	RPA-T8	Biolegend
BV786	CD161	HP-3G10	Biolegend
	CD45RA	HI100	Biolegend
FITC	$\gamma\delta$ TCR	B1	Biolegend
	CD4	RPA-T4	Biolegend
PerCP-Cy5.5	KIR3DL1 - CD158e	DX9	Biolegend
PE	KIR3DL1/DL2 - CD158e/k	5.133	Miltenyi
PE-Dazzle	CCR6	G034E3	Biolegend
	$\gamma\delta$ TCR	B1	Biolegend
PE-Cy5	CD19	HIB19	Biolegend
PE-Cy7	CD56	5.1H11	Biolegend
APC	KIR3DL1/DS1 - CD158e1/2	REA168	Miltenyi
Alexa Fluor 700	CD3	UCHT1	Biolegend
APC-Cy7	KIR2DL5 - CD158f	UP-R1	Miltenyi

RESULTS

Compensation of Spectral Overlap

Proper compensation is critical in high-dimensional fluorescent flow cytometry experiments. In order to correct and compensate for potential spillover errors, UltraComp eBeads were stained with individual conjugated antibodies and used as single-color compensation controls. The beads are around 6 μm in diameter, which is similar in size to that of PBMCs and permits their detection in the flow cytometer. Half of the beads are coated with anti-Fc antibodies that capture fluorescently labeled antibodies upon incubation. The other half is uncoated, providing a negative control in the same tube. In Figure 6A, the emission signals from single stained beads are compared to the autofluorescence control of unstained beads in order to generate a compensation matrix that is then applied to data obtained from cells stained with multiple antibodies. The plots in Figure 6B demonstrate how application of the compensation matrix corrects for fluorescent spillover resulting in the correct identification of CD3+CD19- T-cells and CD3-CD19+ B-cells.

A.



B.

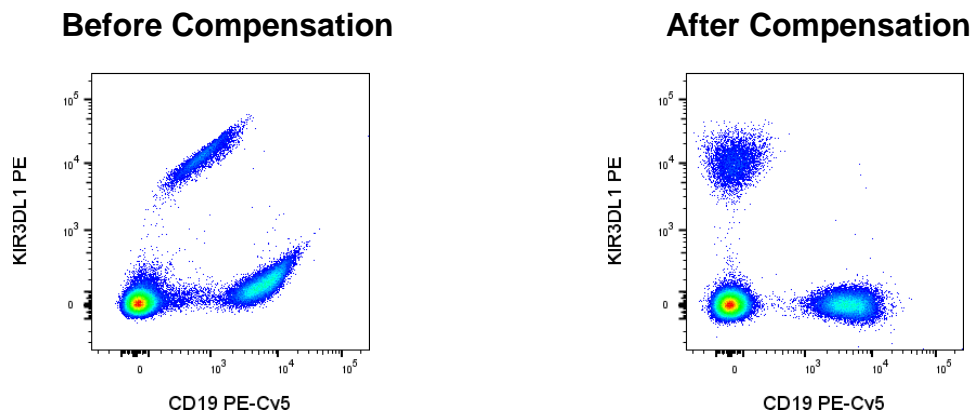


Figure 6. Bead Compensation. **A.** The Alexa Fluor 350 panel consists of cells stained with FVD while the rest of the panels represent a subset of the single stained controls using UltraComp beads stained with individual conjugated antibodies. **B.** The same PBMC specimen before and after application of the compensation matrix.

Flow Cytometry Panel Optimization Using Antibody Titration

Antibody concentrations need to be titrated to determine the minimum concentration of antibody needed to elicit a desired signal and thus maximize the economical use of the antibody resource. By carefully identifying the optimal concentration of antibody and documenting it within our panel, we can assure that our experimental procedures will be consistent and reproducible and will conserve antibody quantity, which allows us to run more experiments.

An antibody cocktail with a starting dilution of 1:100 for each antibody was made and 1:2 serial dilutions were performed to produce antibody cocktails of 1:100, 1:200, 1:400, and 1:800 dilutions. 2×10^6 PBMCs were then stained with the serially diluted antibody cocktails and analyzed. After graphing compensated data as shown in Figure 7, we determined the optimal dilution of antibody by comparing the signal strength to the dilution of antibody used. We chose the smallest antibody dilutions that displayed clear separation of populations, and included them into our flow panel.

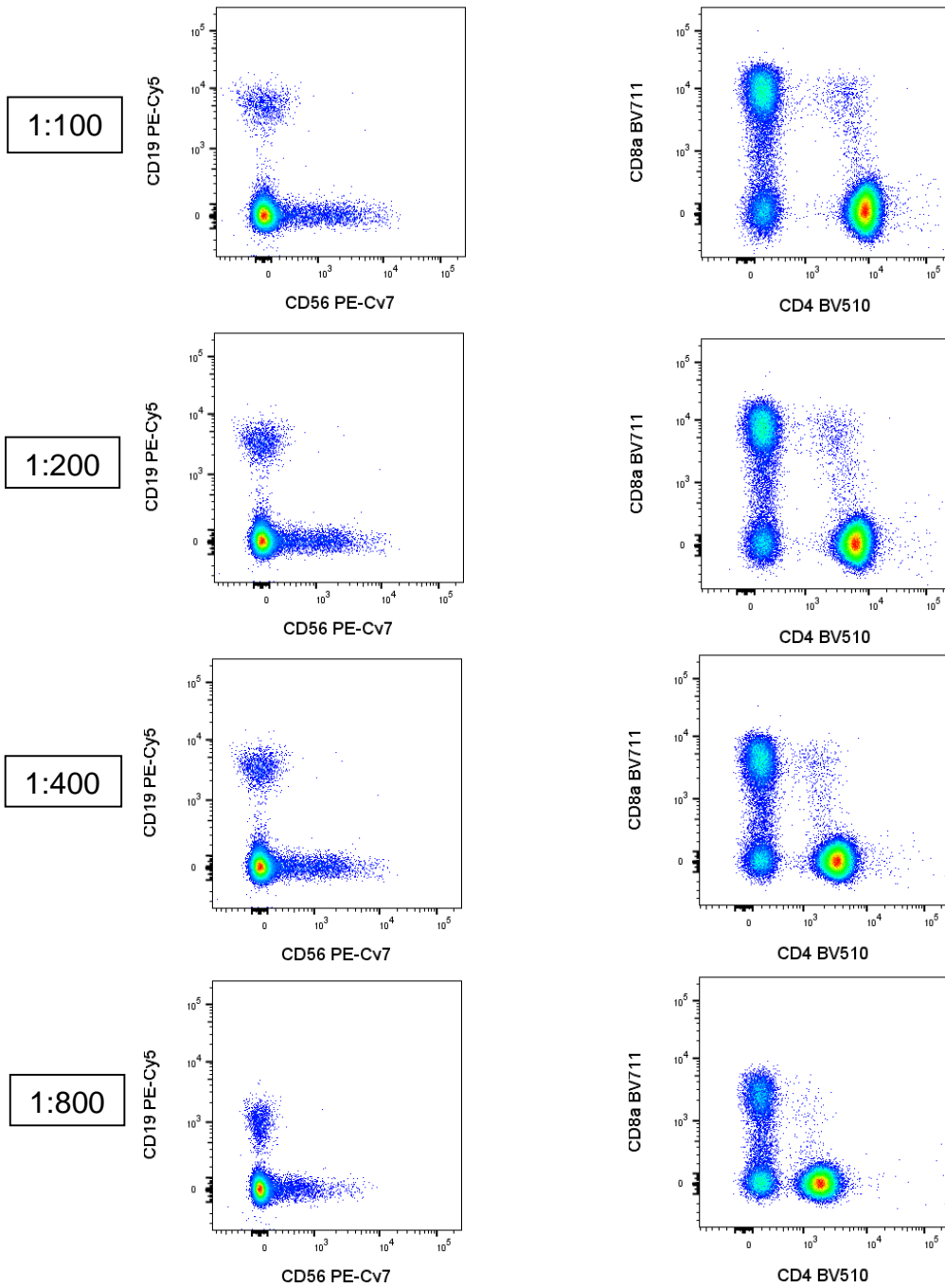


Figure 7. Antibody titration and corresponding fluorescence signal strength.

Cell Surface Panel 1

Laser	Channel	Marker	Clone	Company	Dilution
350 nm	BUV395	Viability			
407 nm	BV421	TCRva24ja18	6B11	Biologend	1:100
	BV510	CD4	OKT4	Biologend	1:500
	BV605	TCRva7.2	3C10	Biologend	1:100
	BV650	CD16	3G8	Biologend	1:200
	BV711	CD8a	RPA-T8	Biologend	1:500
	BV786	CD161	HP-3G10	Biologend	1:100
488 nm	FITC	$\gamma\delta$ TCR	B1	Biologend	1:100
	PerCP-Cy5.5	KIR3DL1	DX9	Biologend	1:100
561 nm	PE	KIR3DL1/DL2	5.133	Miltenyi	1:20
	PE-Dazzle	CCR6	G034E3	Biologend	1:100
	PE-Cy5	CD19	HIB19	Biologend	1:500
	PE-Cy7	CD56	5.1H11	Biologend	1:200
633 nm	APC	KIR3DL1/DS1	REA168	Miltenyi	1:50
	Alexa 700	CD3	UCHT1	Biologend	1:100
	APC-Cy7	KIR2DL5	UP-R1	Miltenyi	1:20

Cell Surface Panel 2

Laser	Channel	Marker	Clone	Company	Dilution
350 nm	BUV395	Viability			
407 nm	BV421	CCR7	G043H7	Biologend	1:100
	BV510	CD4	OKT4	Biologend	1:500
	BV605	HLA-DR	L243	Biologend	1:200
	BV650	CD38	HB7	Biologend	1:100
	BV711	CD8a	RPA-T8	Biologend	1:500
	BV786	CD45RA	HI100	Biologend	1:200
488 nm	FITC	$\gamma\delta$ TCR	B1	Biologend	1:100
	PerCP-Cy5.5	KIR3DL1	DX9	Biologend	1:100
561 nm	PE	KIR3DL1/DL2	5.133	Miltenyi	1:20
	PE-Dazzle	CCR6	G034E3	Biologend	1:100
	PE-Cy5	CD19	HIB19	Biologend	1:500
	PE-Cy7	CD56	5.1H11	Biologend	1:200
633 nm	APC	KIR3DL1/DS1	REA168	Miltenyi	1:50
	Alexa 700	CD3	UCHT1	Biologend	1:100
	APC-Cy7	KIR2DL5	UP-R1	Miltenyi	1:20

Table 2A. Finalized flow panels for cell surface marker staining.

Laser	Channel	Marker	Clone	Company	Dilution
350 nm	BUV395	Viability			
407 nm	BV421	CCR7	G043H7	Biolegend	1:100
	BV510	IL-17A	BL168	Biolegend	1:100
	BV605	HLA-DR	L243	Biolegend	1:200
	BV650	IFN γ	4S.B3	Biolegend	1:100
	BV711	CD8a	RPA-T8	Biolegend	1:100
	BV786	CD45RA	HI100	Biolegend	1:200
488 nm	FITC	CD4	RPA-T4	Biolegend	1:25
	PerCP-Cy5.5	KIR3DL1	DX9	Biolegend	1:100
561 nm	PE	KIR3DL1/DL2	5.133	Miltenyi	1:20
	PE-Dazzle	$\gamma\delta$ TCR	B1	Biolegend	1:100
	PE-Cy5	CD19	HIB19	Biolegend	1:500
	PE-Cy7	CD56	5.1H11	Biolegend	1:200
633 nm	APC	KIR3DL1/DS1	REA168	Miltenyi	1:50
	Alexa 700	CD3	UCHT1	Biolegend	1:100
	APC-Cy	KIR2DL5	UP-R1	Miltenyi	1:20

Table 3. Finalized flow panel for intracellular cytokines post-stimulation. Antibody titrations were carried out with all the antibodies in the experimental flow panel to determine the minimum concentration of antibody to be used in the experiments as shown in the dilution column.

CD4 Downregulation

During the analysis of cytokine expression in different lymphocyte subsets, there was an issue with CD4 downregulation upon stimulation of lymphocytes with PMA/Ionomycin. This downregulation made it impossible to distinguish the CD4+ lymphocytes from the CD4- when the cells were stained with anti-CD4 BV510, the anti-CD4 antibody used in the extracellular marker panels (Figure 8).

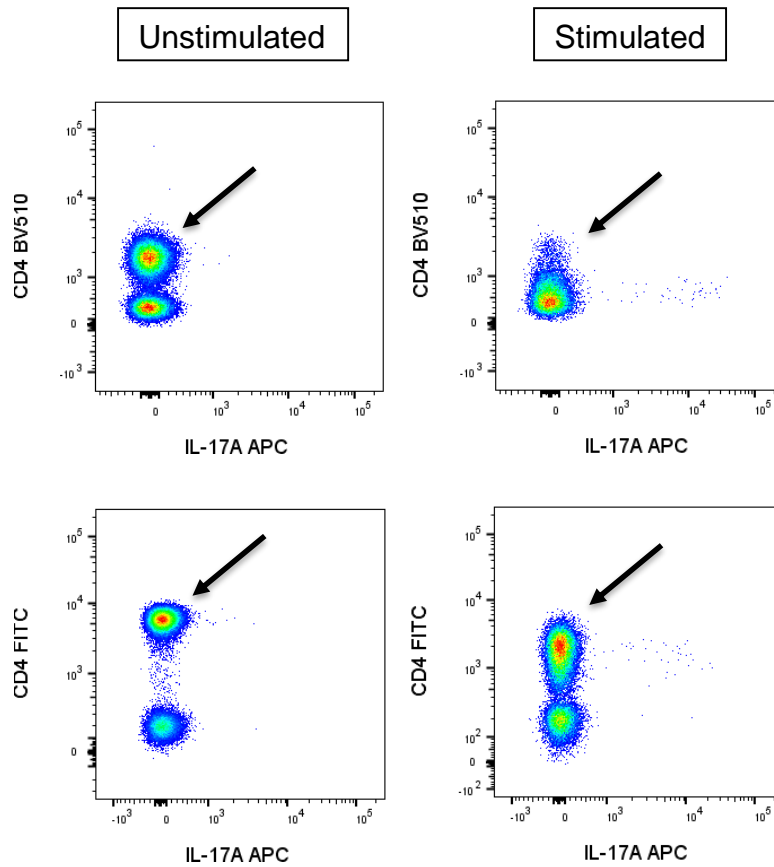


Figure 8. Managing the Problem of CD4 Downregulation. CD4 fluorescence signal in Brilliant Violet 510 (BV510) or fluorescein isothiocyanate (FITC) and the decrease in signal after PMA/Io stimulation. The presence of IL-17A expressing cells demonstrates that the stimulation process was successful.

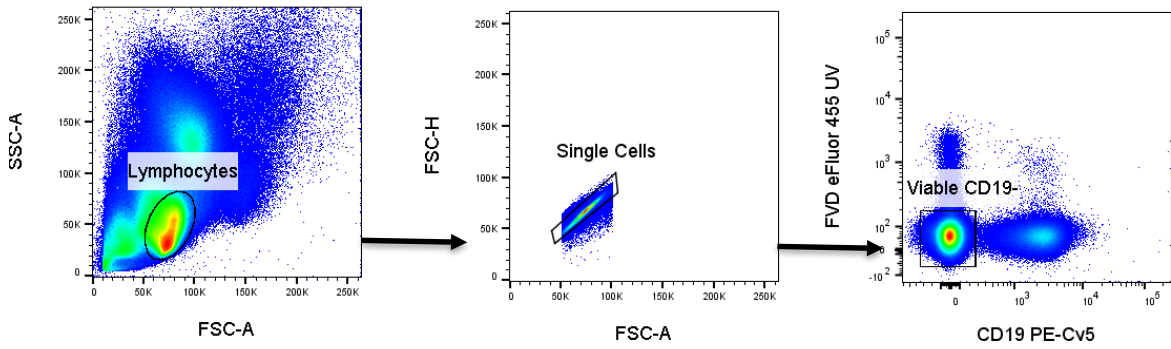
Increasing the concentration of BV510 antibody used could potentially have solved the problem, but due to the high cost of the Brilliant Violet dyes this was not a practical solution. We therefore switched the CD4 marker to a different channel. The anti-CD4 FITC antibody is generally a weaker fluorescent signal than its BV510 counterpart, but it is much cheaper and can be used at much

higher concentrations. By using high concentrations of the FITC antibody, the problem of CD4 downregulation was managed and the flow panel was updated.

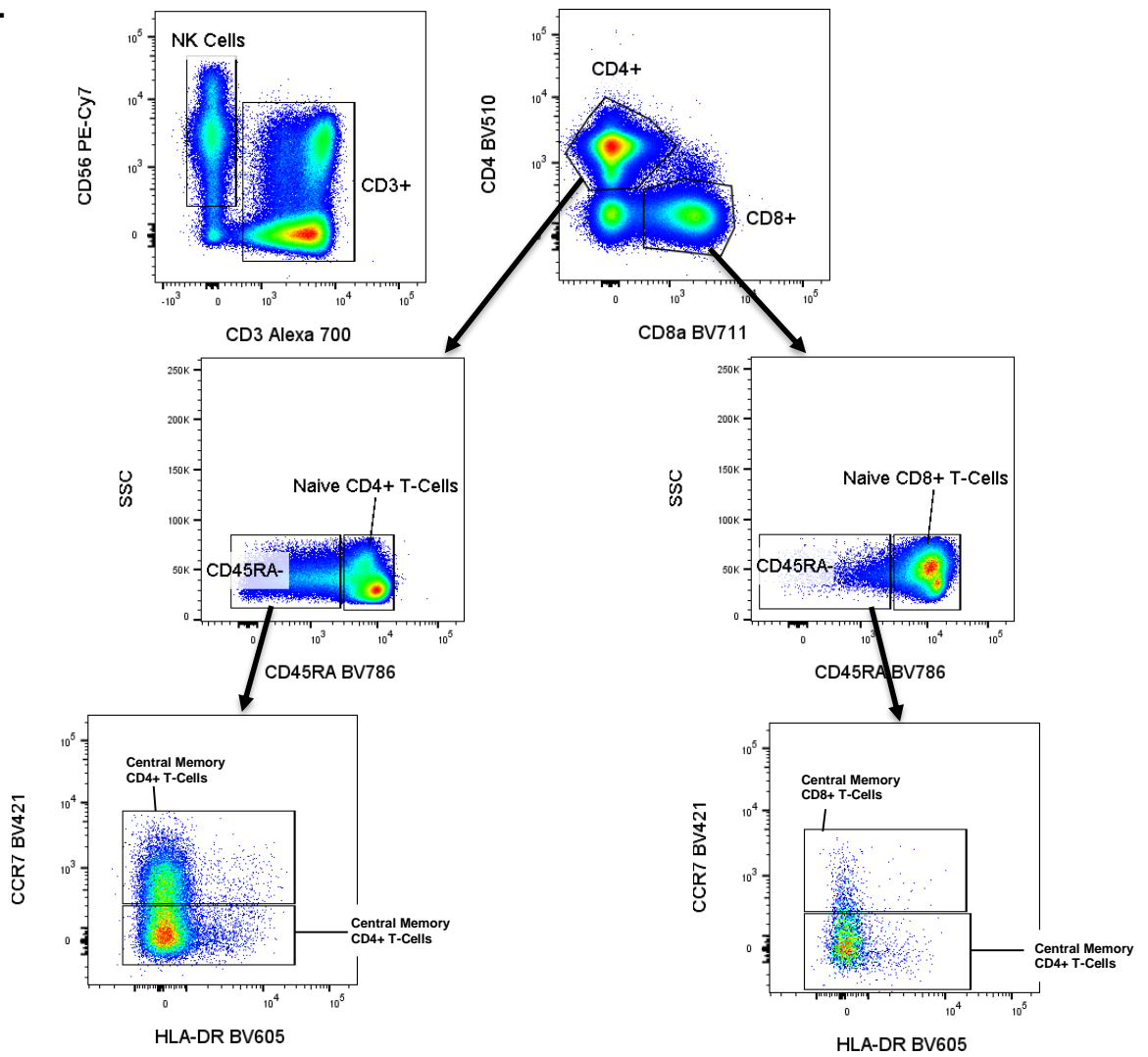
Identification of classic and unconventional lymphocyte subsets

The optimized panels were then applied to PBMCs from a healthy subject to establish the gating strategy to identify important lymphocytes subsets. After compensation, the data set was first cleaned up. This was done by first gating in the lymphocyte population, removing doublet cells, and gating out non-viable or CD19+ B-cells (Figure 9A). From here the NK Cells were identified by gating on CD3-CD56+ cells and the T-cells were identified by gating on CD3+ cells. By looking at the CD3+ cells and gating on CD4+ cells, we can identify the helper T-cells and by gating on CD8+ cells, we can identify the cytotoxic T-cells. By looking at the cytotoxic and helper T-cells respectively, we can gate on CD45RA+ cells to identify the Naïve T-cells. We can then look further at the CD45RA- gate and gate for the CCR7+ central memory T-cells and the CCR7- effector memory T-cells. The unconventional subsets of T-cells can be identified using the same data cleanup strategy shown in Figure 9A. From here, we can gate on the CD3+ cells and from within this gate, we can then gate on $\gamma\delta$ TCR to identify the $\gamma\delta$ T-cells and TCR α 24 β 18 to identify the NK T-cells. Finally, we can look at the $\gamma\delta$ TCR- and TCR α 24 β 18- cells and gate on the CD161+ and TCR α 7.2+ cells to identify the MAIT cells.

A.



B.



C.

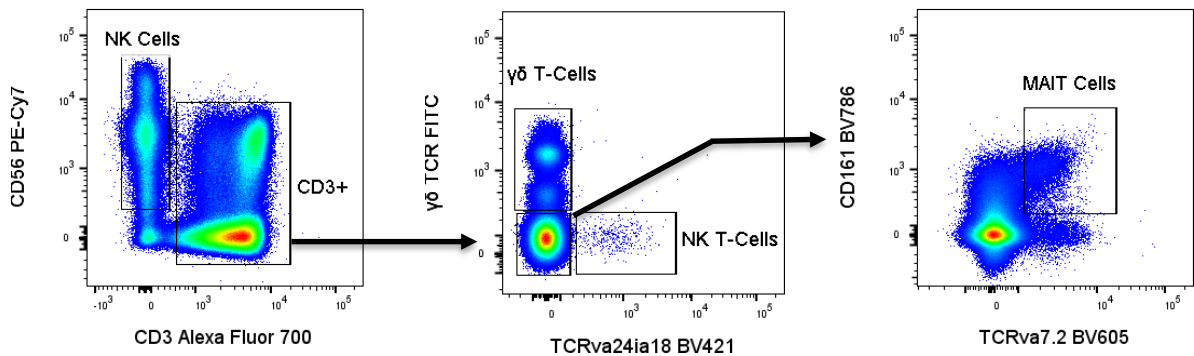


Figure 9. Gating strategy. A. Data cleanup of lymphocytes excluding cell doublets, nonviable cells, and B-cells **B.** Gating of classical lymphocyte subsets **C.** Gating of unconventional lymphocyte subsets.

KIR expression on NK and non-NK cells

The identification of KIRs follows the same data cleanup steps described in Figure 9A in which cell doublets, CD19+, and non-viable cells are gated out. The next step is to gate for the specific cell subsets of interest as described in Figure 9B and 9C. The final step involves gating on the different KIR markers to identify their expression on each of the lymphocyte subsets of interest. By doing this, we were not only able to determine that there is differential KIR expression on different subsets of lymphocytes but also between the cells of different subjects as well (Figure 11).

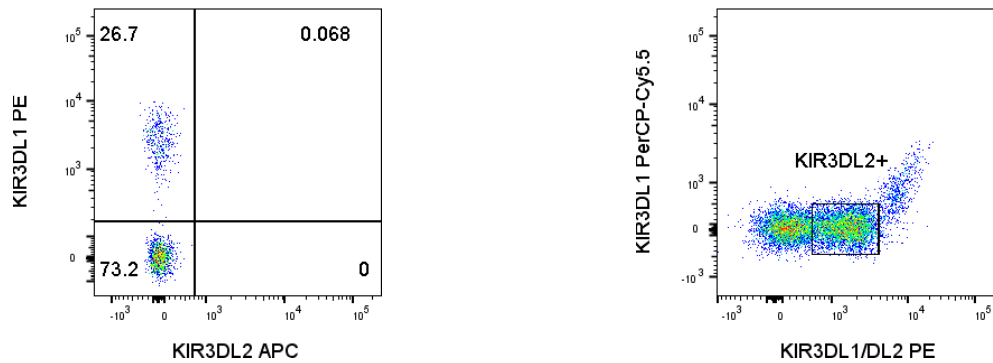
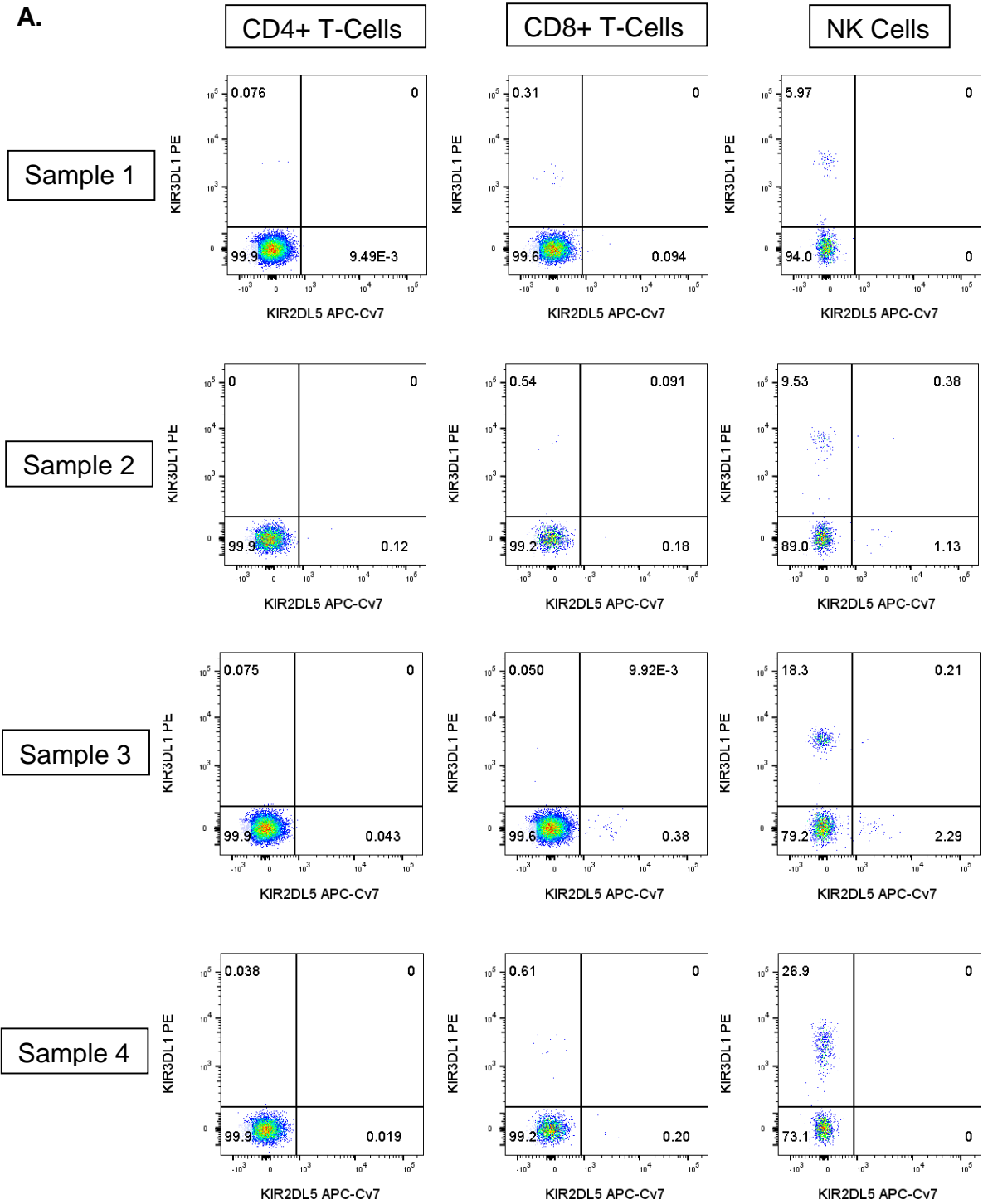


Figure 10. The use of combinatorial staining to identify KIR3DL2+ cells. The KIR3DL2 APC antibody from R&D did not stain properly. Therefore, we stained with anti-KIR3DL1/DI2 and anti-KIR3DL1 to identify cells expressing KIR3DL2.

In our efforts to interrogate the expression of the 4 KIRs we first attempted to use an R&D antibody specific for KIR3DL2 (Clone: FAB2878A), but the antibody failed to stain any cells. By using the gating strategy in Figure 9 to identify NK cells and the data in Figure 10, we were able to identify KIR3DL2+ cells by using a combinatorial staining strategy. This strategy utilizes an antibody (Clone: 5.133) that stains both KIR3DL1 and KIR3DL2 and second antibody (Clone DX9) that identifies KIR3DL1. By plotting KIR3DL1/DL2 vs. KIR3DL1, we can identify the cells that are KIR3DL2+.

A.



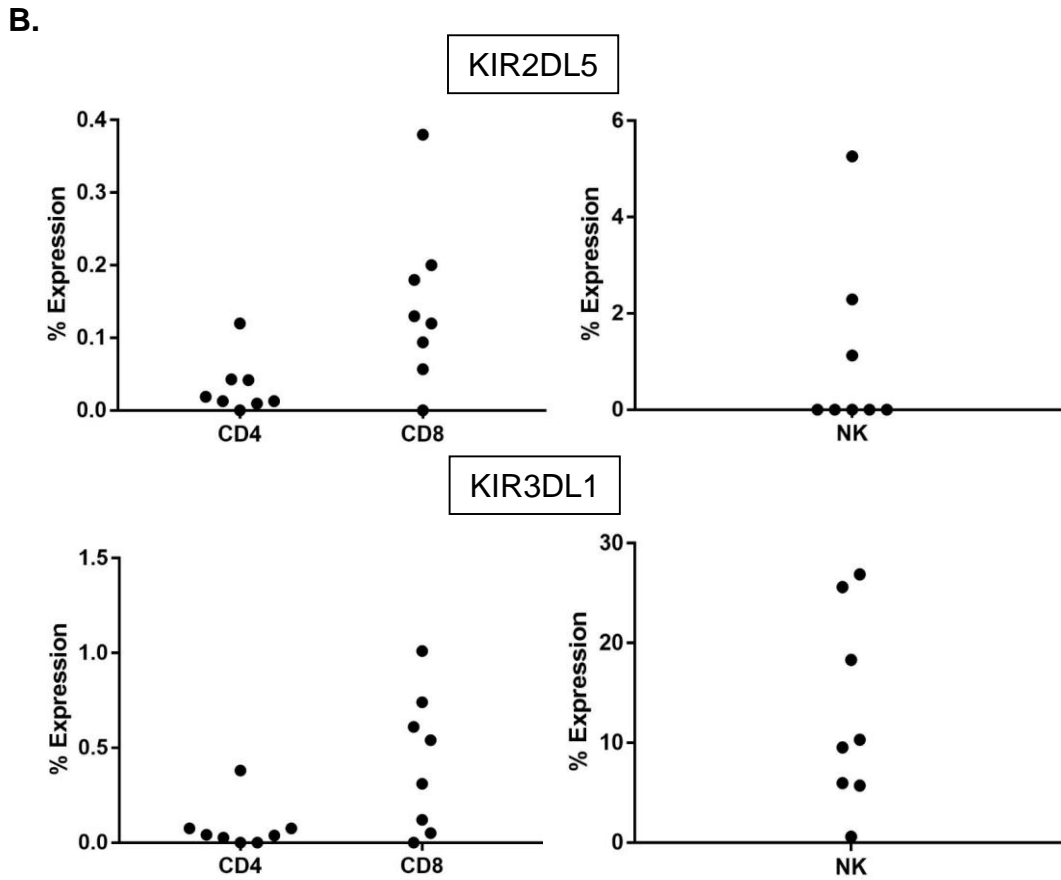


Figure 11. Variable KIR Expression on Different Lymphocyte Subsets. A. Differential expression of KIRs on CD4+ T-cells, CD8+ T-cells, and NK cells from 4 different subjects. **B.** Frequency of KIR3DL1 and KIR2DL5 positive cells amongst CD4+ T-cells, CD8+ T-cells, and NK cells (% Expression).

In sample 1 of Figure 11, we see that less than 0.1% of the CD4+ T-cells express KIR3DL1 or KIR2DL5. We also see that 0.31% of the CD8+ T-cells express KIR3DL1, while around 6% of the NK cells express KIR3DL1. Less than 0.1% of the 3 lymphocyte subsets are KIR2DL5+. In sample 2, around 0.1% of the CD4+ and CD8+ T-cells express KIR2DL5. There is no KIR3DL1 expression on these CD8+ T-Cells, but 0.54% of the CD8+ T-cells express KIR3DL1. 9.53%

of the NK cells express KIR3DL1 and 1.13% express KIR2DL5. In sample 3, less than 0.1% of the CD4+ T-cells express the two KIRS, while 0.38% of the CD8+ T-cells express KIR2DL5. 18.3% of the NK cells express KIR3DL1, while 2.29% of the NK cells express KIR2DL5. In sample 4, less than 0.1% of the CD4+ T-cells express the 2 KIRs. Amongst the CD8+ T-cells, 0.61% express KIR3DL1 and 0.2% express KIR2DL5. 26.9% of the NK cells express KIR3DL1, while there is no expression of KIR2DL5. This data shows how variable the expression of KIRs are on the different subsets of lymphocytes and in between different subjects. Data are summarized in Panel B for 8 healthy subjects.

DISCUSSION

We set out to develop multi-color flow cytometry panels that permit the identification of various lymphocyte subsets as well as expression of IL-17A and IFN γ after in-vitro stimulation. We also wanted to interrogate the expression of 4 KIRs (KIR3DL1, KIR3DS1, KIR2DL5, and KIR3DL2) with the ultimate goal of determining whether differential KIR expression correlates with function in HLA-B27+ versus HLA-B27- subjects.

Antibody titration was performed to choose the optimal concentration of antibody by comparing the signal strengths of each antibody concentration and determining which provided the best signal to background ratio. Tables 1 and 2 show the finalized flow panels. Using 15-color flow cytometry and two panels we can distinguish specific lymphocyte subsets including CD4+ T-cells, CD8+ T-cells, $\gamma\delta$ T-cells, NK cells, NK T-cells, and MAIT cells. In addition, cells expressing 4 AS-relevant KIRs (KIR3DL1, KIR3DS1, KIR2DL5, and KIR3DL2) can be identified.

As shown in Figure 11, we were able to determine that NK cells were not the only lymphocytes that express KIRs, but that CD4+ and CD8+ T-cells also express these KIRs. Notably, KIR expression was most frequent on NK cells, but was still present on both CD4+ and CD8+ T-cells. Although present on all three subsets of lymphocytes, there was substantial variability in the type of KIR expressed on each lymphocyte subset and even further variability between

samples from different subjects. This is consistent with Exley's description of KIR expression.²²

In assembling the three flow cytometry panels, a number of obstacles had to be overcome. First, there was the issue of spectral overlap, which occurs when the fluorescence of a particular dye spills into more channels than the one that is expected to detect the dye's fluorescence.⁴² We were able to account for this problem by applying compensation in our analysis to ensure that the fluorescent signal detected by each channel came from the fluorophore that was getting measured and corrected any potential false positive signal caused by spillover. Second, we observed a downregulation of CD4 upon PMA/Ionomycin stimulation as previously described.⁴⁵ This made it impossible to distinguish the CD4+ population during FACS analysis using the initial choice of anti-CD4 antibody (Anti-CD4 BV510). We solved this issue by using high concentrations of an anti-CD4 FITC antibody to overcome signal loss caused by CD4 downregulation. Third, we attempted to use a commercial antibody specific for KIR3DL2, but the antibody failed to give off any fluorescent signal. At this time, the number of commercially available antibodies specific to individual KIRs is limited, so we had to resort to combinatorial staining strategies. By gating for the KIR3DL1 single marker and the KIR3DL1/DL2 combination marker, we were able to identify two different populations of cells. One of these populations was KIR3DL1 and KIR3DL2 double positive and the other population was positive for only KIR3DL2 as shown in Figure 10. Although we did not have a KIR3DL2

specific antibody, by using this combinatorial staining strategy, we were able to identify a KIR3DL2+ population. As a wider array of reagents becomes commercially available, the analysis of specific KIRs on lymphocyte subsets will become more refined.

Having the multicolor flow cytometry panels described in this thesis available, the next steps would be to analyze PBMC samples from HLA-B27+ and HLA-27- subjects. Such a study should include healthy male and female subjects age 18-65. For every HLA-B27 positive subject, an age and sex-matched HLA-B27 negative control would be identified. Exclusion criteria for the samples would include any diagnosis or history of ankylosing spondylitis, spondyloarthritis, psoriasis, psoriatic arthritis, inflammatory bowel disease, uveitis, HIV infection, and other autoimmune diseases. The goal of the experiment would be to identify how the KIR repertoire on lymphocyte subsets differs between HLA-B27+ and HLA-B27- individuals, and to determine if there is a difference in the function (IL-17A secretion) of these different lymphocyte subsets. The testable hypothesis in this experiment would be that lymphocytes in HLA-B27 positive subjects, expressing KIR3DL1, KIR3DL2, KIR2DL5, or KIR3DS1, differentially produce IL-17A compared with lymphocytes not expressing these KIRs.

Studies in healthy individuals would be followed by the analysis of PBMC specimens from patients with AS. It is feasible that abnormalities in KIR

expression lymphocyte subsets may only become apparent in HLA-B27 positive individuals after the onset of disease.

One potential caveat with regards to the analysis of peripheral blood is that PBMCs may behave differently than tissue resident immune cells specific to each type of tissue. However, biopsy specimens from the spine of patients with AS are extremely difficult to obtain. Another consideration is that although stimulation with PMA/Io mimics TCR activation, in vivo stimulation may lead to different outcomes.

In conclusion, the work presented in this thesis provides the foundation to analyze the expression of AS-relevant KIRs on a variety of lymphocyte subsets and the relationship between KIR and IL-17A expression in both HLA-B27+/HLA-B27- healthy subjects and AS patients. Understanding how KIR expression modulates the production of IL-17A in HLA-B27+ and HLA-B27- subjects will deepen the understanding of AS pathogenesis and may contribute to the development of curative or preventative interventions in AS.

REFERENCES

1. Khan, M. A. *Ankylosing Spondylitis*. (Oxford University Press, 2009).
2. Bowness, P. HLA-B27. *Annual Review of Immunology* **33**, 29–48 (2015).
3. Schlosstein, L., Terasaki, P. I., Bluestone, R. & Pearson, C. M. High association of an HL-A antigen, W27, with ankylosing spondylitis. *New England Journal of Medicine* **288**, 704–706 (1973).
4. Brewerton, D. A. *et al.* Ankylosing spondylitis and HL-A 27. *Lancet (London England)* **1**, 904–907 (1973).
5. Feldtkeller, E., Khan, M. A., van der Heijde, D., van der Linden, S. & Braun, J. Age at disease onset and diagnosis delay in HLA-B27 negative vs. positive patients with ankylosing spondylitis. *Rheumatology International* **23**, 61–66 (2003).
6. Sorrentino, R., Böckmann, R. A. & Fiorillo, M. T. HLA-B27 and antigen presentation: at the crossroads between immune defense and autoimmunity. *Molecular Immunology* **57**, 22–27 (2014).
7. Colbert, R. A., Tran, T. M. & Layh-Schmitt, G. HLA-B27 misfolding and ankylosing spondylitis. *Molecular Immunology* **57**, 44–51 (2014).
8. Asquith, M., Elewaut, D., Lin, P. & Rosenbaum, J. T. The role of the gut and microbes in the pathogenesis of spondyloarthritis. *Best Practice & Research Clinicial Rheumatology* **28**, 687–702 (2014).

9. Abbas, A., Lichtman, A. & Pillai, S. in *Basic Immunology* 39–41 (Elsevier, 2016).
10. Pegram, H. J., Andrews, D. M., Smyth, M. J., Darcy, P. K. & Kershaw, M. H. Activating and inhibitory receptors of natural killer cells. *Immunology and Cell Biology* **89**, 216–224 (2011).
11. Rajalingam, R. Overview of the killer cell immunoglobulin-like receptor system. *Methods in Molecular Biology* 882, 391–414 (2012).
12. Singh, K. M. *et al.* KIR genotypic diversity can track ancestries in heterogeneous populations: a potential confounder for disease association studies. *Immunogenetics* **64**, 97–109 (2012).
13. Cauli, A. *et al.* Killer-cell immunoglobulin-like receptors (KIR) and HLA-class I heavy chains in ankylosing spondylitis. *Drug Development Research* **75 Suppl 1**, S15-19 (2014).
14. Kollnberger, S. *et al.* Interaction of HLA-B27 homodimers with KIR3DL1 and KIR3DL2, unlike HLA-B27 heterotrimers, is independent of the sequence of bound peptide. *European Journal of Immunology* **37**, 1313–1322 (2007).
15. Bowness, P. *et al.* Th17 cells expressing KIR3DL2+ and responsive to HLA-B27 homodimers are increased in ankylosing spondylitis. *Journal of Immunology (Baltimore, Maryland) 1950* **186**, 2672–2680 (2011).
16. Hanson, A. Killer Immunoglobulin-like Receptors Are Associated with Ankylosing Spondylitis. in 2016 ACR/ARHP Annual Meeting: Abstracts.

17. Smith, J. A. & Colbert, R. A. Review: The Interleukin-23/Interleukin-17 Axis in Spondyloarthritis Pathogenesis: Th17 and Beyond. *Arthritis and Rheumatology* **66**, 231–241 (2014).
18. Reveille, J. D. The genetic basis of spondyloarthritis. *Annals of the Rheumatic Diseases* **70 Suppl 1**, i44-50 (2011).
19. Kenna, T. J. *et al.* Enrichment of circulating interleukin-17-secreting interleukin-23 receptor-positive γ/δ T cells in patients with active ankylosing spondylitis. *Arthritis and Rheumatism* **64**, 1420–1429 (2012).
20. Gaffen, S. L., Jain, R., Garg, A. V. & Cua, D. J. IL-23-IL-17 immune axis: Discovery, Mechanistic Understanding, and Clinical Testing. *Nature Reviews. Immunology* **14**, 585–600 (2014).
21. Baeten, D. *et al.* Secukinumab, an Interleukin-17A Inhibitor, in Ankylosing Spondylitis. *New England Journal of Medicine* **373**, 2534–2548 (2015).
22. Exley, M. A., Tsokos, G. C., Mills, K. H. G., Elewaut, D. & Mulhearn, B. What rheumatologists need to know about innate lymphocytes. *Nature Reviews. Rheumatology* **12**, 658–668 (2016).
23. Maecker, H. T., McCoy, J. P. & Nussenblatt, R. Standardizing immunophenotyping for the Human Immunology Project. *Nature Reviews. Immunology* **12**, 191–200 (2012).
24. Gulzar, N. & Copeland, K. F. T. CD8+ T-cells: function and response to HIV infection. *Current HIV Research* **2**, 23–37 (2004).

25. Nepom, G. T. MHC class II tetramers. *Journal of Immunology (Baltimore Maryland 1950)* **188**, 2477–2482 (2012).
26. Lubberts, E., Koenders, M. I. & van den Berg, W. B. The role of T-cell interleukin-17 in conducting destructive arthritis: lessons from animal models. *Arthritis Research & Therapy* **7**, 29–37 (2005).
27. Glanville, N. *et al.* $\gamma\delta$ T cells suppress inflammation and disease during rhinovirus-induced asthma exacerbations. *Mucosal Immunology* **6**, 1091–1100 (2013).
28. Vivier, E. *et al.* Innate or Adaptive Immunity? The Example of Natural Killer Cells. *Science* **331**, 44–49 (2011).
29. Brennan, P. J., Brigl, M. & Brenner, M. B. Invariant natural killer T cells: an innate activation scheme linked to diverse effector functions. *Nature Reviews. Immunology* **13**, 101–117 (2013).
30. Chua, W.-J. *et al.* Polyclonal MAIT Cells Have Unique Innate Functions in Bacterial Infection. *Infection and Immunity* IAI.00279-12 (2012).
doi:10.1128/IAI.00279-12
31. Delves, P. *Essential Immunology*. (Roitt, 2006).
32. Miyahira, A. Types of immune cells present in human PBMC | Sanguine Bio Researcher Blog. *Sanguine Biosciences* (2012). Available at:
<http://technical.sanguinebio.com/types-of-immune-cells-present-in-human-pbmc/>. (Accessed: 20th February 2017)

33. Liu, C. Characterization of ionomycin as a calcium ionophore. (1978).
Available at: <http://www.jbc.org/content/253/17/5892.abstract>. (Accessed: 21st February 2017)
34. Flow Cytometry - Semrock. *Semrock* Available at:
<https://www.semrock.com/flow-cytometry.aspx>. (Accessed: 1st March 2017)
35. Herzenberg, L. A. *et al.* The history and future of the fluorescence activated cell sorter and flow cytometry: a view from Stanford. *Clinical Chemistry* **48**, 1819–1827 (2002).
36. Herzenberg, L. A., Tung, J., Moore, W. A., Herzenberg, L. A. & Parks, D. R. Interpreting flow cytometry data: a guide for the perplexed. *Nature Reviews Immunology* **7**, 681–685 (2006).
37. Julius, M. H., Masuda, T. & Herzenberg, L. A. Demonstration that antigen-binding cells are precursors of antibody-producing cells after purification with a fluorescence-activated cell sorter. *Proceedings of the National Academy of Sciences of the United States of America* **69**, 1934–1938 (1972).
38. Chattopadhyay, P. K. & Roederer, M. Cytometry: today's technology and tomorrow's horizons. *Methods (San Diego California)* **57**, 251–258 (2012).
39. Lundsten, K. BioLegend Video - Brilliant Violet™ Webinar Featuring Kelly Lundsten. *Biolegend.com* (2012). Available at:
http://www.biolegend.com/brilliantviolet_webinar. (Accessed: 20th February 2017)

40. Chattopadhyay, P. K. *et al.* Brilliant violet fluorophores: a new class of ultrabright fluorescent compounds for immunofluorescence experiments. *Cytometry Part J International Society of Analytical Cytology* **81**, 456–466 (2012).
41. Picot, J., Guerin, C. L., Le Van Kim, C. & Boulanger, C. M. Flow cytometry: retrospective, fundamentals and recent instrumentation. *Cytotechnology* **64**, 109–130 (2012).
42. Roederer, M. Compensation in flow cytometry. *Current Protocols in Cytometry* **Chapter 1**, Unit 1.14 (2002).
43. Flow Cytometry Facility - Compensation. *Medical University of South Carolina*
Available at: <http://regmed.musc.edu/flowcytometry/Compensation.html>.
(Accessed: 24th February 2017)
44. Colbert, R. A. & Ward, M. M. 17 and 23: prime numbers for ankylosing spondylitis? *Lancet (London England)* **382**, 1682–1683 (2013).
45. Hasan, M. *et al.* Semi-automated and standardized cytometric procedures for multi-panel and multi-parametric whole blood immunophenotyping. *Clinical Immunology* **157**, 261–276 (2015).

CURRICULUM VITAE

